Egyptian Geophysical Society
EGS Journal, Vol. 13, No. 1, 35-44 (2015)

AEROMAGNETIC DATA INTERPRETATION TO DELINEATE FAULTS AT GABAL AL-JURUF AREA, CENTRAL EASTERN DESERT, EGYPT

S.O. Elkhateeb[(1)], S.R. Salem[(1)], A.M. Eldosouky[(2)]

(1) Department of Geology, Faculty of Science, South Valley University, Egypt.
(2) Environmental Researcher, Dababya Protectorate, Ministry of State for Environmental Affairs, Egypt.

تفسير البيانات المغناطيسية الجوية لتحديد الفوالق المدفونة فى منطقة جبل الجرف وسط الصحراء الشرقية فى مصر

الخلاصة: يقوم هذا العمل على تحليل البيانات المغناطيسية لمنطقة جبل الجرف وسط الصحراء الشرقية، مصر لرسم التراكيب السطحية والتحتسطحية. تعتمد الطريقة على معالجة البيانات المغناطيسية الجوية لتحديد الفوالق الجيولوجية المدفونة. تم تأكيد الفواصل الجيولوجية باستخدام طريقتي المشتقة الرأسية وسلسلة الاستمرار لأعلى لبيانات الشدة المغناطيسية الكلية وذلك عن طريق تحديد المشتقة المائلة ومعدل التدرج الأفقي. تم تطبيق طريقة أويلر على بيانات الشدة المغناطيسية الكلية لتحديد عمق الفواصل. من تحليل هذه النتائج تم تحديد أعماق الفواصل على مستويات مختلفة لمنطقة الدراسة. من تفسير البيانات المغناطيسية أظهرت النتائج أن هذه المنطقة متأثرة بعدة تراكيب تحتسطحية معظمها يأخذ اتجاهات شمال شمال غرب– جنوب جنوب شرق، شمال غرب– جنوب شرق، شمال– جنوب غرب. وهناك بعض الاتجاهات السطحية الموجودة بالمنطقة وهي شمال– جنوب وشرق–غرب.

ABSTRACT: *The present work is based on the analysis of the total magnetic intensity map of Gabal El-Juruf area, Central Eastern Desert, Egypt to delineate surface and deep faults. Our technique consists of processing aeromagnetic data, so as to highlight the buried geological contacts. The study of the geological contacts is ensured by the first vertical derivative and upward continuation processing of total magnetic intensity map at various altitudes, followed by the determination of the tilt derivative and horizontal gradient magnitude for each altitude. Also, Euler deconvolution technique has been applied for total magnetic intensity map to determine depth to contacts. These results allow the determination of the contact systems for the survey area at each level. The interpretation of magnetic data indicates that the study area is affected by many subsurface structural trends. The NNW-SSE, NW-SE and the NE-SW are the major surface lineament trends. Other trends defined through the interpretation of magnetic data include the N-S direction and E-W direction. Most of these lineament trends are at shallow depths.*

INTRODUCTION

The area under study is located in the northern part of Central Eastern Desert, Egypt. The area extends from latitudes 27º 00’ to 27º 21’E and longitudes 32º 40’ to 33º 16´ 43’’ N in the central eastern desert, Egypt as shown in fig (1).

The study area can be reached from the famous Hurghada City on the Red Sea coast, through a desert track passing through W. Bali and then northward to the track of W. El Attrash. The area is arid, very hot in summer and cold in winter. Cultivation and natural vegetation are scarce, except some grasses and scattered trees.

The magnetic method is frequently used to search for buried magnetic materials (Walsh, 1989). Another common application for the determination of the probable depth to basement beneath sedimentary rocks. The location of shallow magnetic materials such as buried container, pipes, metals debris are also enhanced with magnetic data processing together with enhancement procedures which substantially improve the interpretations of the magnetic data(Birch, 1984) .

2. Geological Setting:

The geological map of the study area (Fig. 2) is covered mainly by recent wadi deposits and gravel fills of Quaternary age and a group of Mesozoic formations that include Qusier Clastic Member, Taref sandstone Member, Wata Formation and Galala Formation units at the western part. Meanwhile the Central and Eastern parts of the area are covered by Precambrian basement Rocks including: Metagbbro-Diorite Complex, Alkali feldspar granite, trachytic dykes, Hammamat group, Dukhan Volcanics, Geosynclinal Metavolcanics, (geological map of the Gebel El Urf Quadrangle, Egypt, 1983).

3. Structural Setting:

In general, the basement rocks, in the Eastern Desert, lie within the foreland folds and thrust bell of the Pan-African Orogeny. It is exposed in a series of swells along two geoanticlines trending in NNW - SSE, and coinciding merely with Idfu-MarsaAlam and Qena - Safage roads (El Gaby et al., 1988).For chronological and structural considerations, it was divided by Stern et al, (1985) into three domains,Southern, Central and Northern Eastern Desert (i.e. SED, CED and NED). SED and CED are characterized by the ophiolites and ophioliticmelanges with minor Late to Post-orogenicplutonisms, low angle thrusts of NW - SE direction and the right lateral shears (e.g. Qena - Safaga Road), with the Najjd fault systems in the northern part of the CED which overprinted the ancient low angle thrusts but are absent in the SED and that is the only difference between these two terrains.

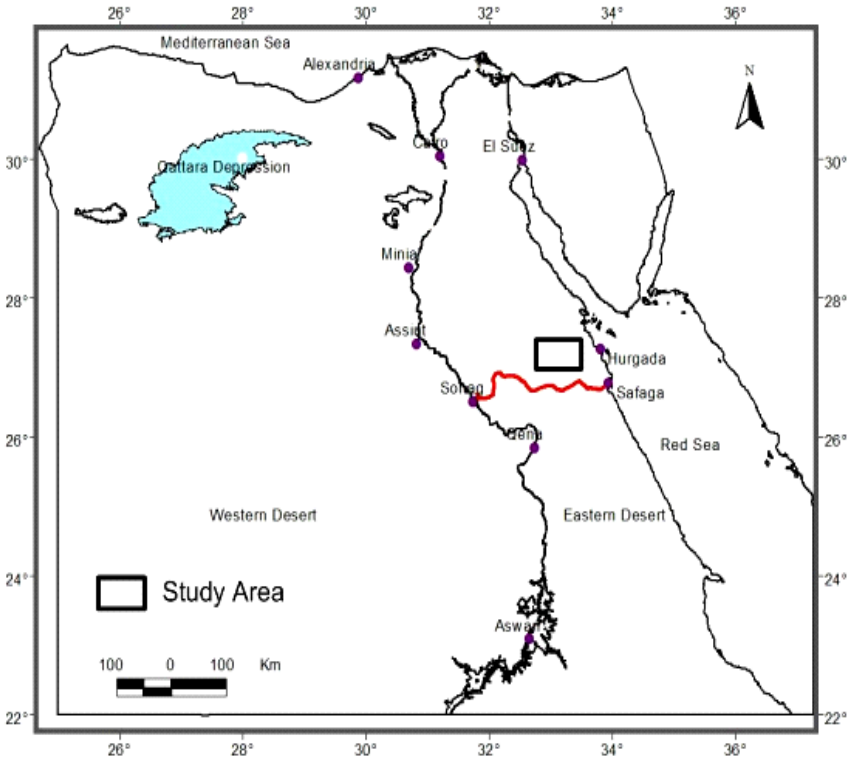

Fig. (1): Location map of the study area.

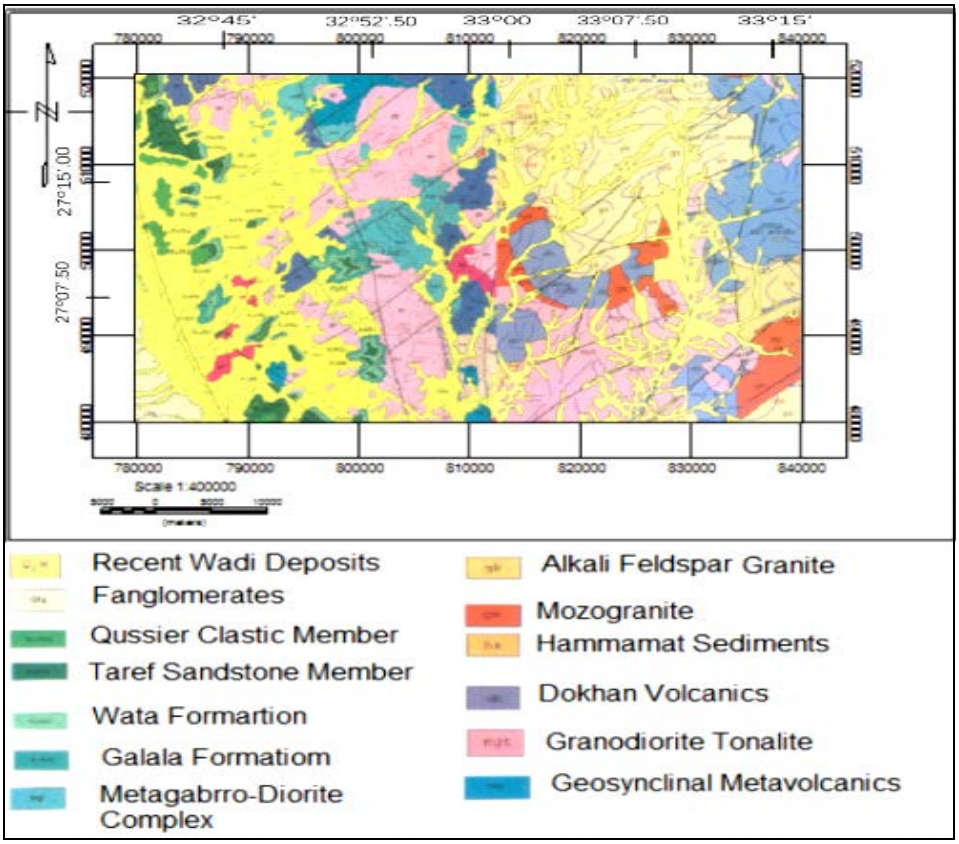

Fig. (2): Geologic map of the study area (modified after EGSMA, 1983).

Stern et al, 1985 concluded that the Najjd NW-SE oriented strike-slip faults are strongly related to the NE SW oriented normal faults characterize the NED with widespread Late and Post-orogeni granitic plutonisms which have relatively younger age than their equivalents in the SED. Other fractures such as the N – S and E - W are less frequent in the SED and CED but have considerable foundation in the NED.

Ayoub (2003) studied the geology and radioactivity of the different basement rocks exposed in G. Um Tweir area that lies to the north of the investigated area. He classified the rocks of the area from oldest to youngest into; metavolcanics, quartz diorites, Dokhanvolcanics, Hammamat sediments, gabbro-granophyre associations, younger granites and post granitic dykes. The same author mentioned that the three significant joint and fault sets predominant in the area are NE-SW, NW- SE and E-W for the joints, and NE-SW, N-S and ENE-WSW for the faults.

4. MATERIALS AND METHODS

4.1. Aeromagnetic data:

The magnetic data used in this study was obtained from the Egyptian Mineral Resources Authority collected by Aero Service Company (1983). Aeromagnetic surveys were flown with a flight height of 120 m and the average magnetic inclination was 39.5 N and declination was 2 E.

The total magnetic intensity (TMI) map (Fig. 3) was deduced by subtracting the theoretical geomagnetic field or IGRF (International Geomagnetic Reference Field).

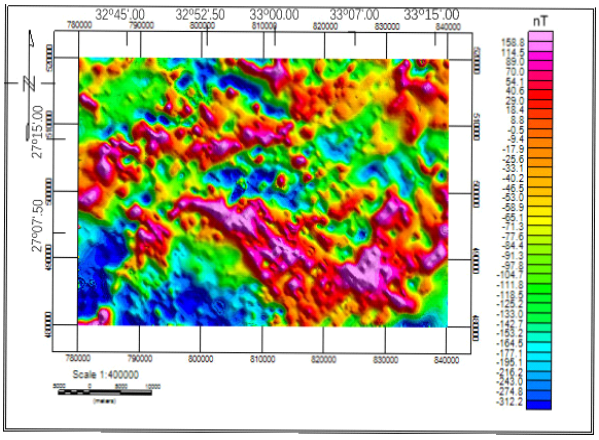

Fig. (3): Total magnetic intensity (TMI) map of the study area.

4. 2. Methods:

For the purpose of this study, many interpretation methods were applied with the final goal of enhancing the signature of hidden faults, contacts and edges or boundaries of magnetic sources. The estimation of the locations of these structural discontinuities was achieved firstly by the application of First Vertical Derivative, Horizontal gradient magnitude, and Tilt derivative of the total magnetic intensity data and the upward continuation at various altitudes (2, 4, 6 km). Finally, Euler deconvolution is applied to the total magnetic intensity data to detect contact depths of the area.

4.2.1. First Vertical Derivative (FVD):

This enhancement is designed to look at fault and contact features. The first vertical derivatives can be mathematically derived from the final total magnetic field anomaly map, and it can be measured directly when using a gradiometer instrument for taking measurements over the surveyed area. The first vertical derivatives are of particular use in sharper resolution of near-surface features. Practical procedures for determination of the derivatives involve taking average values over circles at different distances from a grid point and the process is repeated for each grid point (Sharma, P.V, 1997).In the present study, the total magnetic intensity map (Fig. 3) is processed to produce the FVD map (Fig. 6).

4.2.2. Horizontal Gradient Magnitude (HGM)

Horizontal Gradient Magnitude (HGM) method (Blakely and Simpson, 1986,

Nasreddine and Haydar, 2001) is perhaps the simplest approach of estimating magnetic contact locations and depths because it does not require the calculation of vertical derivatives but only the calculation of the two first-order horizontal derivatives of the field. Thus, the HGM is given by:

HG(x,y) =

$$\sqrt{\left(\frac{\partial M}{\partial X}\right)^2+\left(\frac{\partial M}{\partial y}\right)^2}\sqrt{\left(\frac{\partial M}{\partial X}\right)^2+\left(\frac{\partial M}{\partial y}\right)^2}$$

Where $\partial M/\partial x$ and $\partial M/\partial y$ are the field gradients in the x (East) and y (North) directions respectively.

HGM is applied to TMI map (Fig. 5) and to every upward continuation map at altitudes of 2, 4, & 6 km(Figs:9a,9b, & 9c) respectively.

4.2.3. Tilt Derivative (TD):

The tilt derivative (TDR) is defined by Miller and Singh (1994) as the arc tangent of the ratio of a vertical to a combined horizontal derivative:

$$TDR = \tan^{-1}\left(\frac{VDR}{THDR}\right) TDR = \tan^{-1}\left(\frac{VDR}{THDR}\right)$$

Where VDR and THDR are the first vertical and total horizontal derivatives of the TMI respectively. While VDR can be positive or negative, THDR is always positive.

The principal objective of TDR is to delineate the vertical and horizontal edges of concealed magnetic structures (zero contour line = contact location). Theoretical studies of the TDR applied to the magnetic models are presented by Cooper and Cowan (2006); Fairhead et al., (2004), Verduzco et al., (2004), Salem et al. (2007, 2008).

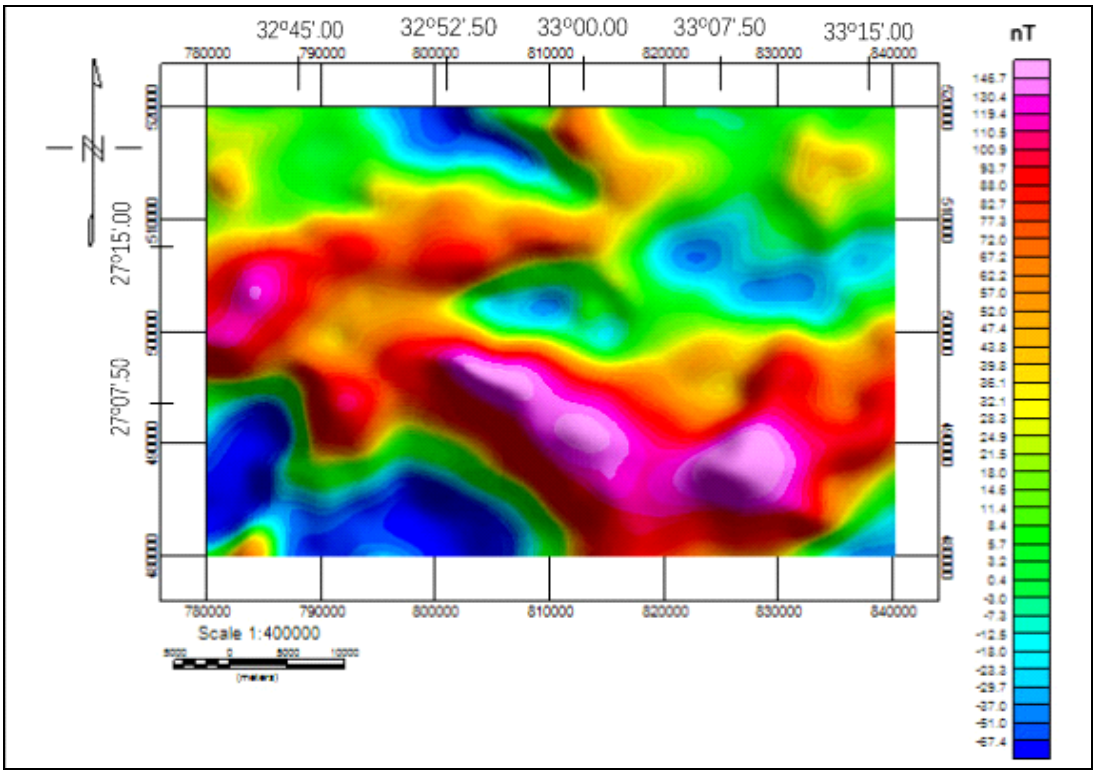

Fig. (4a): Upward continuation map of TMI map at altitude of 2 km.

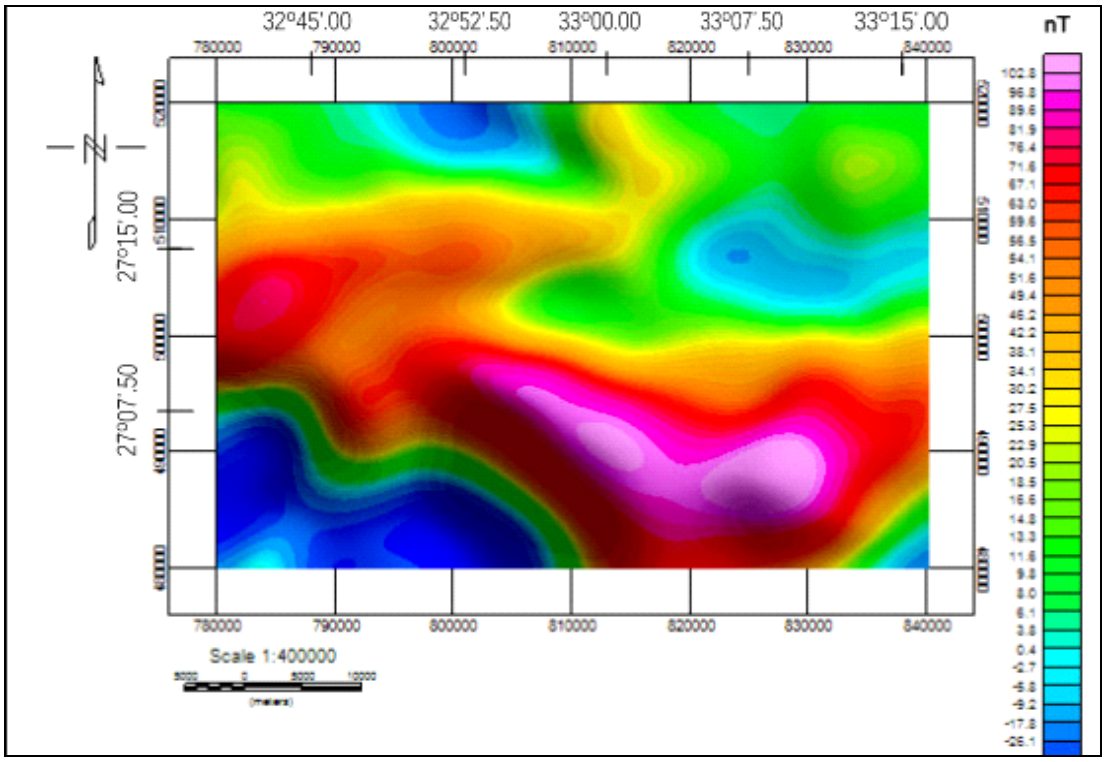

Fig. (4b): Upward continuation map of TMI map at altitude of 4 km.

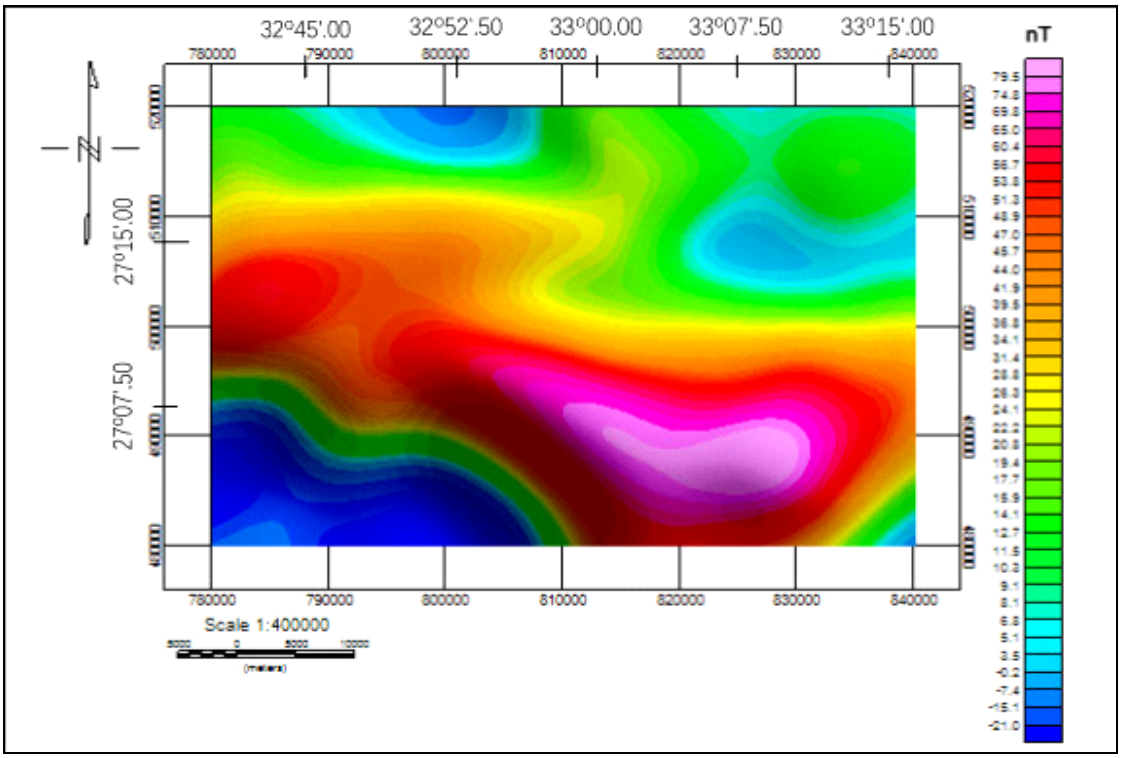

Fig. (4c): Upward continuation map of TMI map at altitude of 6 km.

TD is applied to TMI map (Fig. 7) and to every upward continuation map at altitudes of 2, 4, & 6 km (Figs:10a,ab, & 10c) respectively.

4.2.4. Upward Continuation:

Upward continuation is considered a clean filter because it produces almost no side effects that may require the application of other filters or processes to correct. It minimizes the effects of shorter-wavelength (higher wave number) components associated with more local, shallower anomaly sources; thus it can be used as an effective smoothing technique for the separation of anomalies due to deeper sources.

Also, upward continued data may be interpreted numerically and with modeling programs. This is not the case for many other filter processes. Geosoft formula to calculate upward continuation is:

$$L(r) = e^{-hr}$$

Where (h) is the distance in ground units, to continue up relative to the plane of observation and (r) is the wavenumber (Dobrin M. B., Savit C. H., 1988).

Upward continuation is applied to TMI map at altitudes of 2. 4, & 6 km (Figs:4a, 4b, & 4c) respectively.

4.2.5. Euler Deconvolution:

The objective of the Euler deconvolution process is to produce a map showing the locations and the corresponding depth estimations of geologic sources of magnetic or gravimetric anomalies in a two-dimensional grid (Reid, 1990). Of many depth estimation techniques, the Euler deconvolution has become a popular choice because the method assumes no particular geological model. However, the conventional approach to solving Euler equation requires tentative values of the structural index (SI) preventing it from being fully automatic and assumes a constant background that can be easily violated if the singular points are close to each other (Dewangan, P., T. Ramprasad, M.V. Ramana, Desa, M., and Shailaja, B. 2007).

In general, the unknown regional field (B) can be approximated using Taylor series as:

$$B_{(x,y)} = B_0 + x\frac{\partial B}{\partial x} + y\frac{\partial B}{\partial y} + 0(2),$$

Where B_0 is the constant background at the center of the specified window and O (2) represents higher-order terms in the Taylor series expansion. The anomalous field (T), can now be expressed as the difference between the observed (F) and regional (B) fields.

$$F = (x - x_0)\frac{\partial(F-B)}{\partial x} + (y - y_0)\frac{\partial(F-B)}{\partial y} + (z - z_{z0})\frac{\partial(F-B)}{\partial z} + n(F-B) = 0$$

Euler equation becomes nonlinear and is solved linearly by assuming tentative values of the SI (Thompson, D. T, 1982; Reid, A. B et al., 1990). The Euler equation can also be solved linearly assuming constant background (Gerovska et al., 2005). Euler deconvolution is applied to TMI map (Fig.8).

5. RESULTS AND INTERPRETATION

5.1. Contact locations from the total magnetic intensity map:

Inspection of the preparedhorizontal gradient magnitude map (Fig.5) from the original data showed that a lot of structural trends can be observed in NE, NW,ENE and WNW directions with some minor NS and EW directions. It is worth to note that the high frequencies of the anomalies produced by these trends are indicative for their shallow depth of the causative sources.

First vertical derivative of original total magnetic intensity map (Fig. 6) show perfect match with HGM results.

On the other hand, to ensure the obtained results the tilt derivative map (Fig. 7) has been constructed and revealed nearly the same structural patterns observed previously from the horizontal gradient map but with somewhat more tight clusters of anomalies and indicating shallow depths of sources as experienced from the obvious zero contour lines on the map.

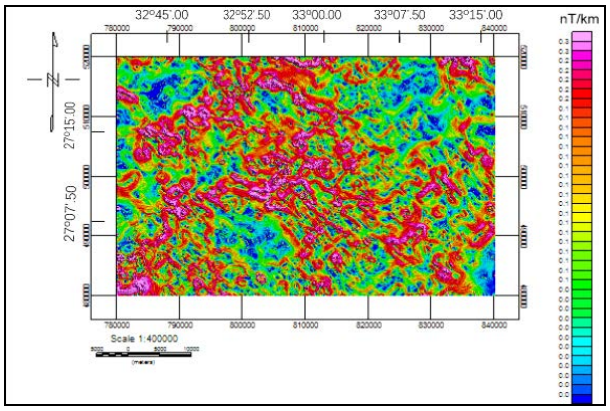

Fig (5): Horizontal gradient magnitude (HGM) of (TMI) map.

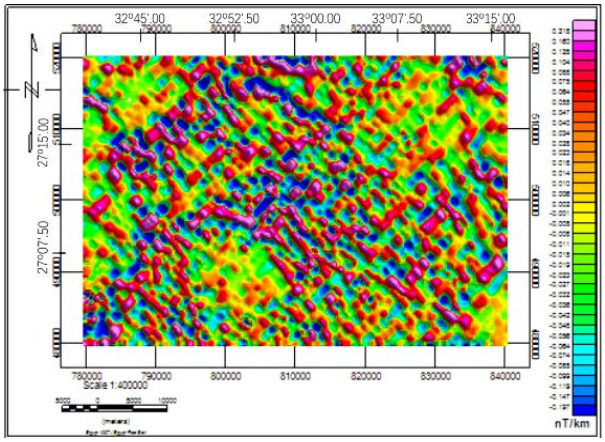

Fig. (6): First vertical derivative map of TMI.

The standard Euler deconvolution was applied to the total magnetic intensity map. For interpreting contacts, faults, structural index of 1 was found to give the best results (Fig.8). The results showed range of depths between 0.449 and 1.430km with trends of NW-SE, NNW-SSE, & NE-SW directions. These results confirm the idea that the structural trends of the study area are indicative for their shallow depths of the causative sources.

5.2. Contact locations from upward continuation maps:

Again, to delineate at the locations and depths of the obtained structural trends and to ensure their probable continuity with depth, upward continuation of the original data has been carried out at three altitudes 2, 4, 6 km (Fig:4a, 4b,&4c).

Critical examination of the constructed horizontal gradient magnitude (Figs: 9a, 9b, & 9c) and tilt derivative maps (Figs:10a, 10b, & 10c) showed that the obtained trends exhibit a regional nature and express evidently the contacts between the rock units, and the residual nature of these trends obtained from the original data have disappeared ensuring the illustrated shallow depths.

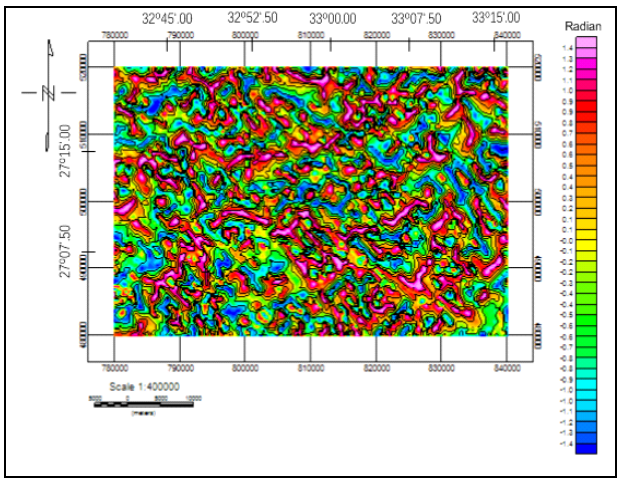

Fig. (7): Tilt derivative map of TMI map.

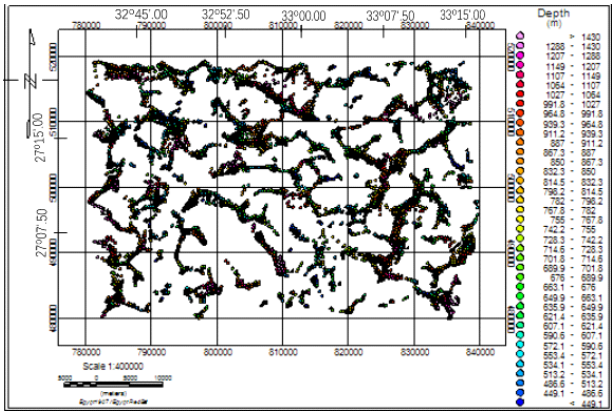

Fig. (8): Euler deconvolution of TMI with SI = 1.

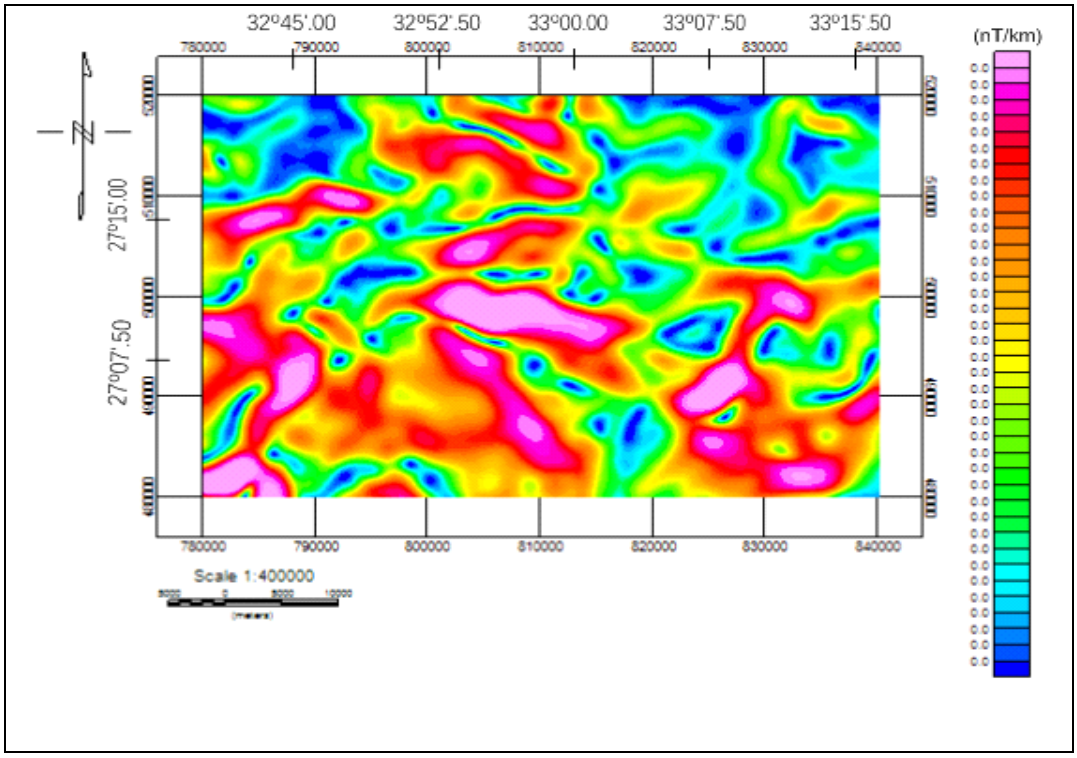

Fig. (9a): Horizontal gradient magnitude map of upward continuation map at altitude of 2 km.

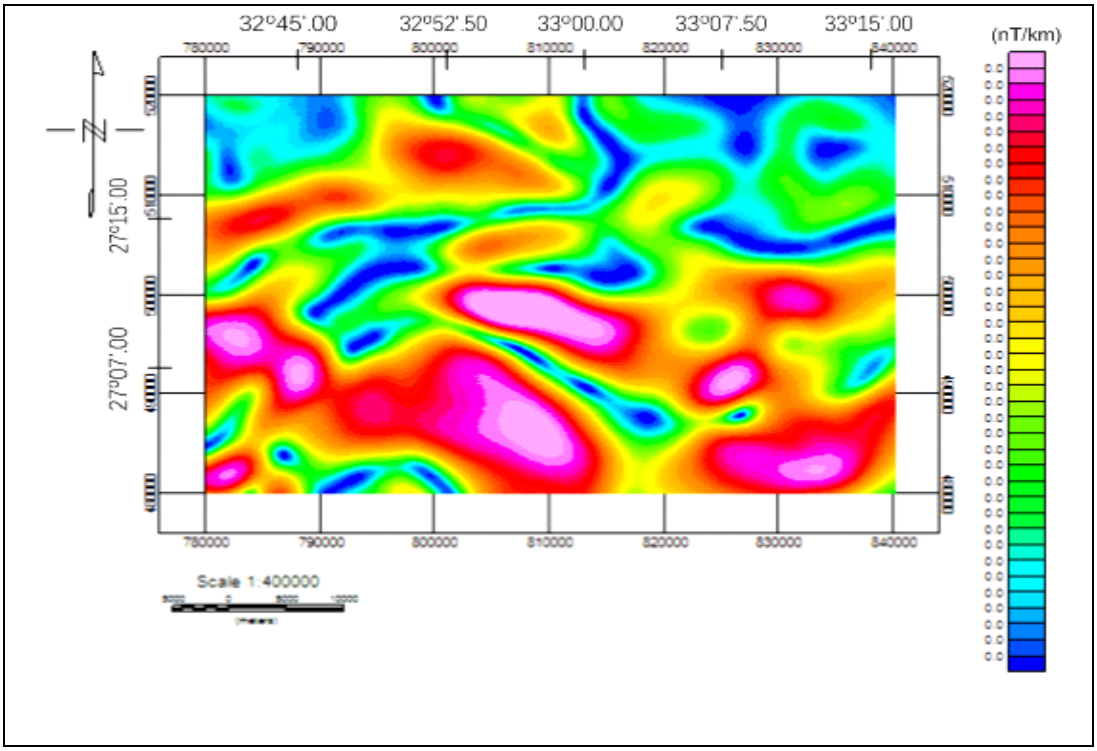

Fig. (9b): Horizontal gradient magnitudemap of upward continuation map at altitude of 4 km.

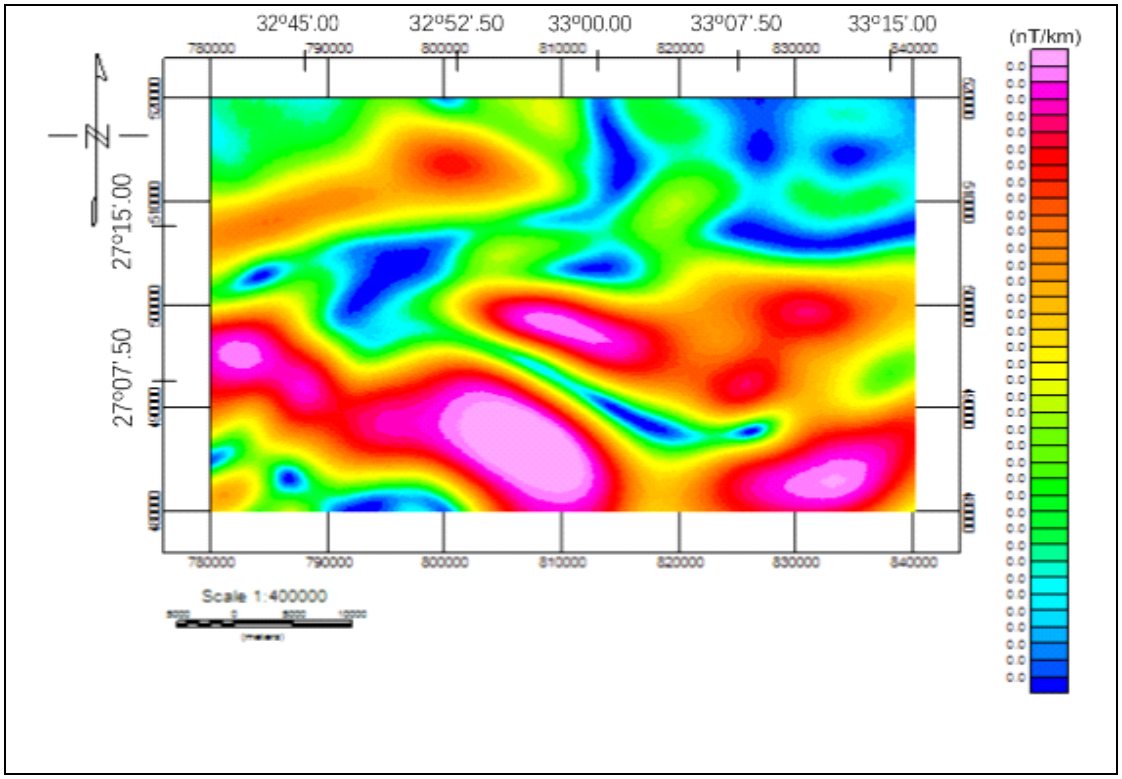

Fig. (9c): Horizontal gradient magnitudemap of upward continuation map at altitude of 6 km.

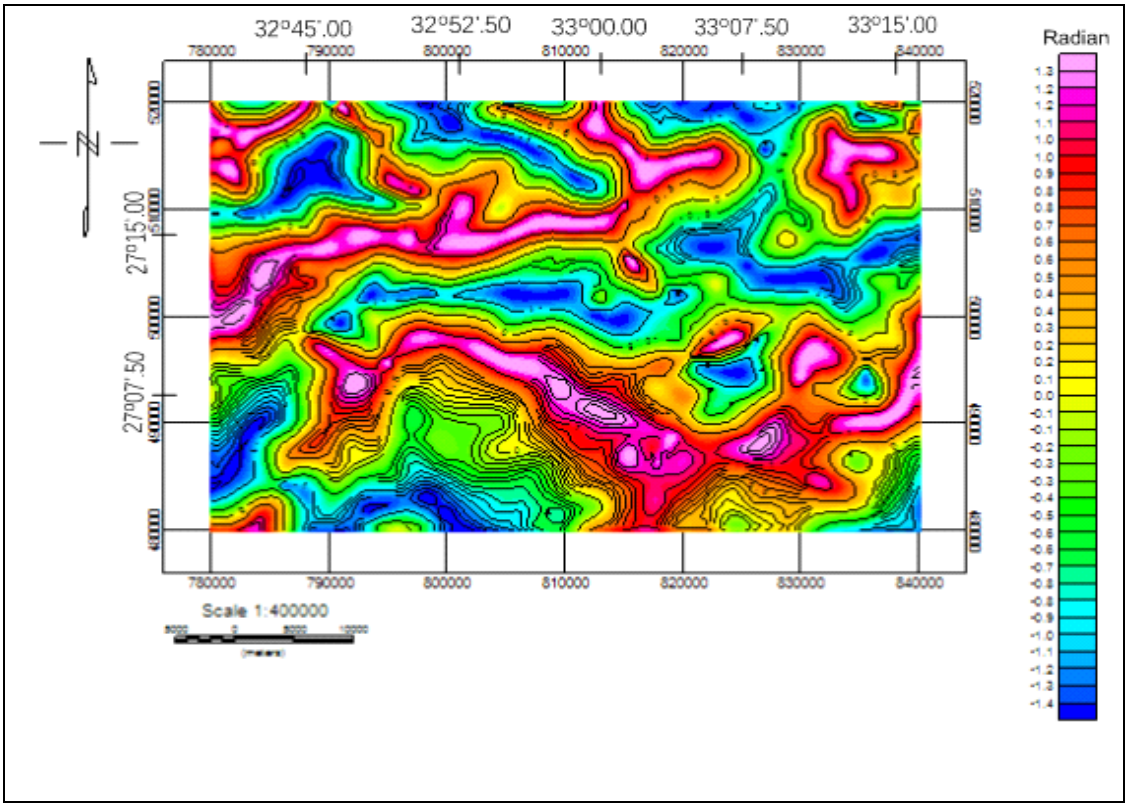

Fig. (10a): Tilt derivative map of upward continuation map at altitude of 2 km.

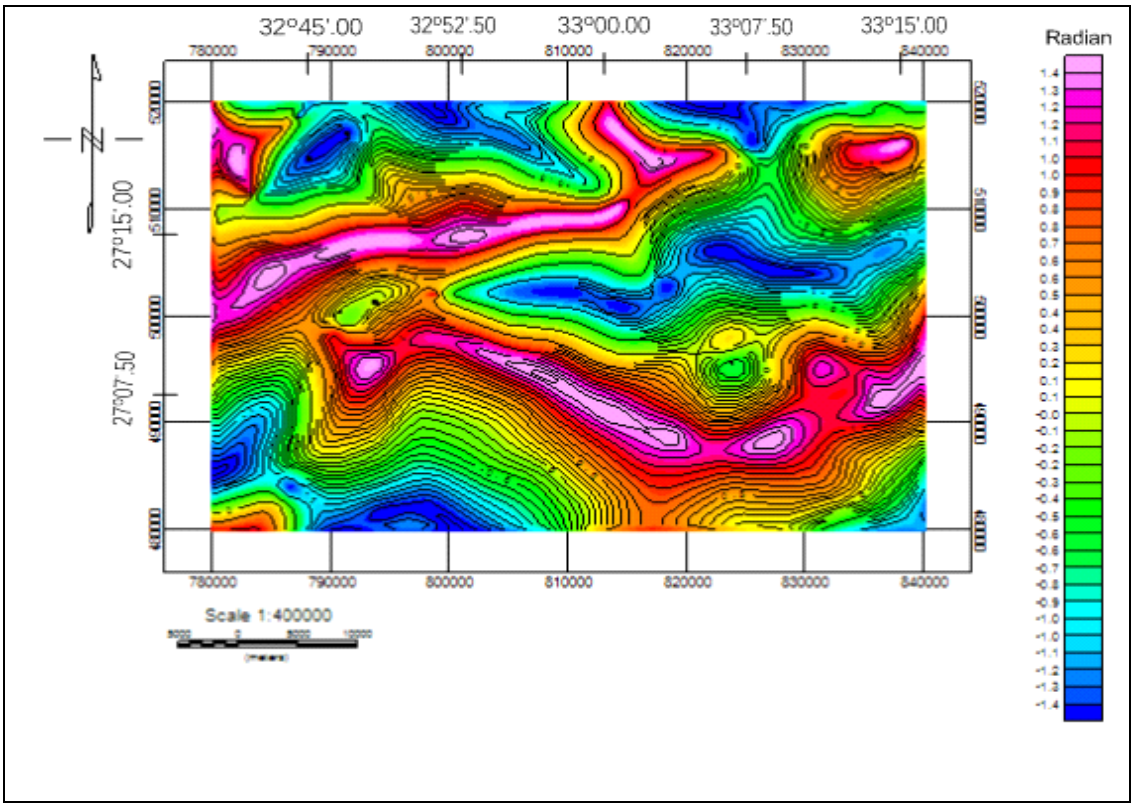

Fig. (10b): Tilt derivative map of upward continuation map at altitude of 4 km.

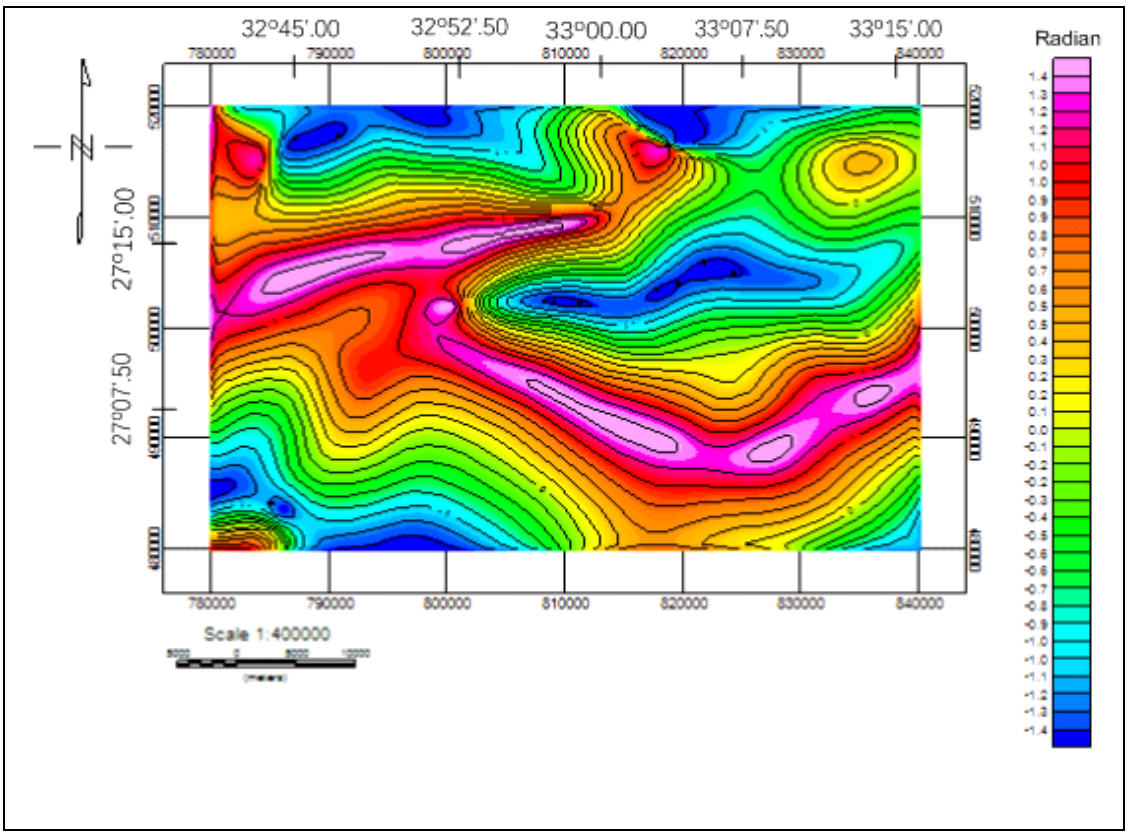

Fig. (10c): Tilt derivative map of upward continuation map at altitude of 6 km.

6. CONCLUSION

The tilt derivative, first vertical derivative, Euler deconvolution, and horizontal gradient magnitude of total magnetic intensity map over the study area define shallow contact locations. The upward continuation process shows the attenuation of short-wave length anomalies with respect to the increase in the observation to source distance. The tilt derivative and horizontal gradient magnitude of upward continuation at various altitudes indicate deep seated structural contact locations.

As a general conclusion it can be said that the predominant structural trends in the study area have a residual nature and therefore exhibit shallow depths. The fact that can be obtained through the following steps after upward continuation confirmed these results with a more regional appearance of the trends in the form of contacts between the rock units.

REFERENCES

Ayoub, R.R., (2003), Geology and radioactivity of Gabal Um Tweir area, Eastern Desert, Egypt, PH.D. Thesis, Cairo University, Egypt, p. 286.

Birch, F.S. (1984). Bedrock Depth Estimates from Ground Magnetometer Profiles.Groundwater, v. 22(4), p.427-432.

Blakely, R.J. and Simpson, R.W. (1986), Approximating edge of source bodies from magnetic or gravity anomalies. Geophysics, v. 51, pp. 1494 -1498.

Cooper, G.R., Cowan, D.R. (2006), Enhancing potential field data using filters based on the local phase. ComputGeosci 32:1585–1591.

Dobrin, M.B., Savit, C.H. (1988), Introduction to geophysical prospecting 4th edn, McGraw Hill book company, New York.

Dewangan, P., T. Ramprasad, M.V. Ramana, Desa, M., and Shailaja, B. (2007), Automatic interpretation of magnetic data using Euler deconvolution with nonlinear background, Pure and Applied Geophysics, Vol.164; 2359-2372p.

El-Gaby, S., List, F.K., and Tehrani, R. (1990): The basement complex of the Eastern Desert and Sinai of Egypt. In Said, R.(ed.), The Geology of Egypt ; Balkema, Rotterdam, pp. 175-184.

El-Gaby, S. and Greiling, R.O., (eds) (1988), The Pan-African Belt of Northeast Africa and Adjacent Areas.Tectonic Evolution and Economic Aspects of a Late Proterozoic Orogen.vi + 369 pp. Braunschweig, Wiesbaden: Vieweg&Sohn; marketed and distributed by John Wiley & Sons. Price £53.05 (hard covers). ISBN 3 528 06325 4.

Fairhaed, J.D., Green, C.M., Verduzco, B. and Mackenzie, C., (2004), A new set of magnetic field derivatives for mapping mineral prospects. 17th ASEG Geophysical Conference and Exhibition, Sydney, Australia, Expanded Abstract.

Geological map of the Gebel El Urf Quadrangle, Egypt, 1983, Scale 1 : 250 000, EGSMA.

Geological map of Hurghada Quadrangle, Egypt, 2005, Scale 1 : 250 000, EGSMA.

Gerovska, D., Stavrev, Y. and Arauzo-Bravo, M.J. (2005), Finite-difference Euler deconvolution algorithm applied to the interpretation of magnetic data from northern Bulgaria, Pure App. Geophys. 162, 591-608.

Miller, H.G., and Singh, V. (1994), Potential field tilt: a new concept for location of potential field sources. J. Appl. Geophys., 32:213-217.

Nassreddine, B. and Haydar, A.B., (2001), Interpretation of magnetic anomalies using the horizontal gradient analytical signal. Annali Di Geofisica, v. 44, pp. 505-526.

Reid, A.B., Allsop, J.M., Granser, H., Millet, A.J. & Somerton, I.W. (1990), Magnetic interpretations in three dimensions using Euler deconvolution Geophysics, 55, 80-91.

Salem, A., Williams, S., Fairhead, J.D., Ravat, D., Smith, R. (2007), Tilt depth method, a simple depth estimation method using first-order magnetic derivatives. SEG Leading Edge 26/12:1502–1505.

Salem, A., Williams, S., Fairhead, D., Smith, R., Ravat, D., (2008), Interpretation of magnetic data using tilt-angle derivatives. Geophysics 73:L1–L10.

Sharma, P.V. (1997), Environmental and Engineering Geophysics, Cambridge University Press.

Stern, R.J. and Hedge, C.E. (1985), Geochronologic and isotopic constraints on Late Precambrian crustal evolution in the Eastern Desert of Egypt. American Journal of Science, v.285, p. 97-127.

Thompson, D.T. (1982), EULDPH: A new technique for making computer-assisted depth estimates from magnetic data,Geophys. 47, 31–37.

Verduzco, B., Fairhead, J.D., Green, C.M., Mackenzie, C. (2004), New insights into magnetic derivatives for structural mapping. Lead Edge 23:116–119.

Walsh, D.C. (1989). Surface geophysical exploration for buried drums in urban environments applications in New York City in Proc of the Third Nat Outdoor Action Conf. on Aquifer Restoration, Groundwater Monitoring and Geophysical Methods, Orlando 935-949.